24. Change of Loss-cone due to the Electric Field on CHS

M. Osakabe, S. Okamura, K. Ida, S. Kubo, T. Minami, Y. Yoshimura, K.Tanaka
H. Idei, M. Isobe, K. Matsuoka, and CHS group

National Institute for Fusion Science, Toki-shi, Gifu 509-5292, Japan

1. Introduction

The confinement of fast ions are one of the most important issues in the study of magnetically confined fusion devices. In toroidal helical systems, the radial electric field plays an important role on the topology of particle orbit, hence affects the formation of loss-cones[1]. Many theoretical and numerical works concerning on this issue are performed [2,3,4,5]. The experimental studies on the E_r-induced loss-cones are reported by Kurimoto,*et. al.,*[6] and Zushi,*et.al.*[7]

During High Power/High-Ti experimental campaign on CHS, a drastic change of the ion temperature measured by Neutral Particle Analyzer (T_i^{NPA}) was observed when the ECH was superposed on low density NBI-plasmas, although no significant change was observed on the ion temperature measured by Charge Exchange Recombination Spectroscopy (T_i^{CXRS}). The NPA spectra of ECH superposed NBI (NBI+ECH) discharge are compared to those of NBI only discharges.

In this article, the experimental results and initial analysis on the NPA-spectra of these discharges are reported.

2. Experimental Set-Up

A Neutral Particle Analyzer is used to measure the $\psi_{cx}(E)$. Since the E_r-induced loss-cone affects the confinement of large pitch-angle particles, the measurements were focused on two viewing angle locations as shown in Fig.1. The one is 12-degree location, which correspond to perpendicular sight line to magnetic field, and the other is 38-degree location which correspond to parallel sight line.

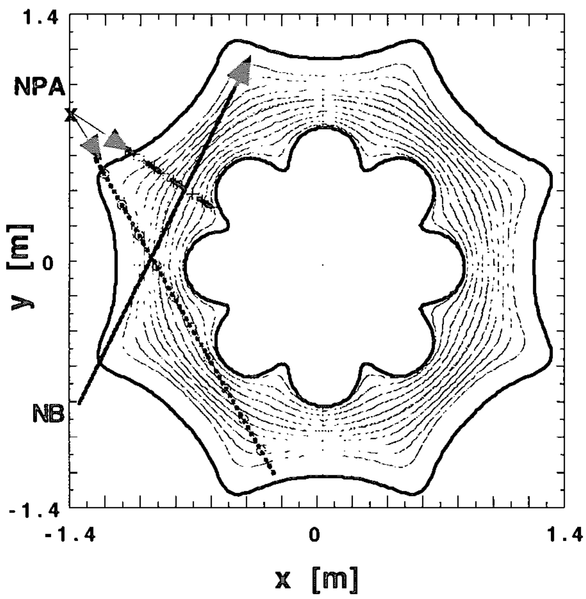

Fig. 1 Sight line of NPA. Short-dashed lines with open circles show the perpendicular (12-degree) sight line, w the long-dashed lines with crosses does the parallel one.

The electric-field was determined from

plasma rotation measurement using Charge Exchanged Recombination Spectroscopy.

In the experiment, low density high-Ti mode plasmas are sustained by the co.-injected Neutral Beam (Fig. 2). The Electron Cyclotron Heating(53GHz/106GHz) is superposed on this plasma during t= 60-80ms. The electron density rise is slightly suppressed during this phase. As is mentioned, the T_i^{NPA}, which is obtained by the perpendicular measurements, jumps up to 450-eV from 300-eV.

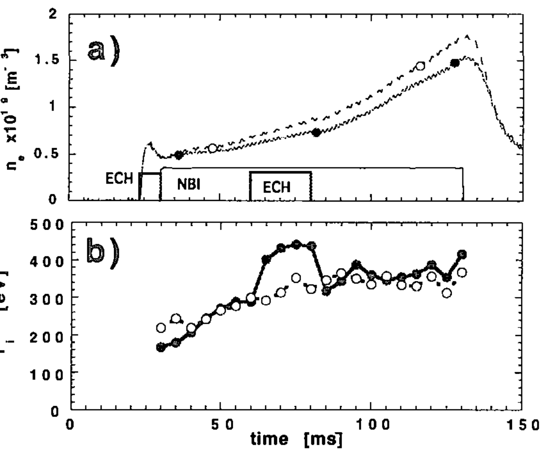

Fig. 2 Typical time trace of (a) electron density ar during NBI- and NBI+ECH- discharges. The dashed lines with closed circles sl forms for NBI-discharge, while the solid lines with open circles show wave forms f NBI+ECH discharges.

3. Results and Remarks

Figure 3 show the NPA-spectra obtained between t=60-80ms. Figure 4(a) shows the corresponding T_i-profile measured by CXRS. The small peaks at 2-keV in parallel NPA-spectra are the contribution from 1/18-energy component of NB. The parallel spectra are similar both in the NBI- and NBI+ECH-discharges, while, in the perpendicular spectra, an enhancement of the charge exchange flux around 2-keV is observed for NBI+ECH-dischrges. There are three explanations for this enhancement of $\psi_{cx}^{perp.}$ in NBI+ECH-discharges. (1) The enhancement of pitch angle scattering due to the change of the T_e and/or Z_{eff}. (2) The enhancement of neutral and/or ion density as a source of measured charge exchanged neutral flux. (3) The enhancement of confinement property of the ions on the NPA sight line.

Although the Z_{eff} is not monitored, the effect of Z_{eff} is considered to be low as impurity

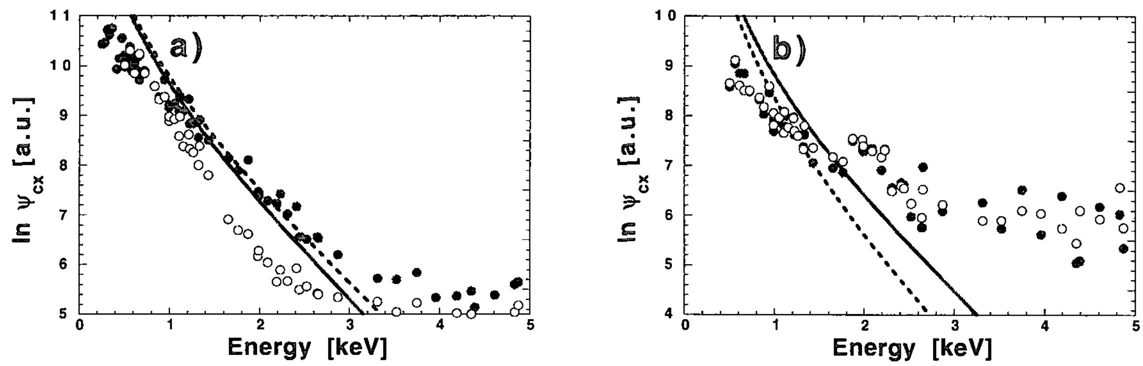

Fig. 3 Measured NPA spectra between t= 60 - 80ms. (a) Spectra on perpendicular line of sight, and (b) tl parallel line of sight. The open and the closed circles show the spectra of NBI-and NBI+ECH-discharges, respectively. The solid-lines show the estimated NPA spectrum for NBI+ECH-discharges by using measu and Ti- profiles, while the dashed lines do that for NBI-discharges. The neutral densities are evaluated f PROCTOR-code.

ions tend to be pumped out by ECH. As a result Z_{eff}-effect on the pitch angle scattering is expected to be reduced. Although the electron temperature is higher in the ECH superposed discharges than in NB-only discharges, it is unlikely to occur the enhancement of pitch angle scattering in this energy range. Since the electron temperatures are 0.5-keV for NBI-discharges and 2.8-keV for NBI+ECH-discharges and the critical energy is in the range of 10-40keV, the enhancement in pitch angle scattering will likely to occur in higher energy range.

The effect of plasma parameters on the ψ_{cx}^{perp} is evaluated by estimating the NPA spectra using the measured $n_e(\rho)$-, $T_e(\rho)$- and $T_i(\rho)$-profiles. The neutral density profiles are obtained from the PROCTOR-code analysis. The $n_i(\rho)$ is assumed to be same as $n_e(\rho)$ in the evaluation. The solid- and dashed- lines in Fig. 3 show the evaluated NPA-spectra for NBI+ECH- and NBI-discharges, respectively. No significant differences is found in the perpendicular spectra between these two discharges. The difference in plasmas parameters will not explain the enhancement of ψ_{cx}^{perp} around 2-keV.

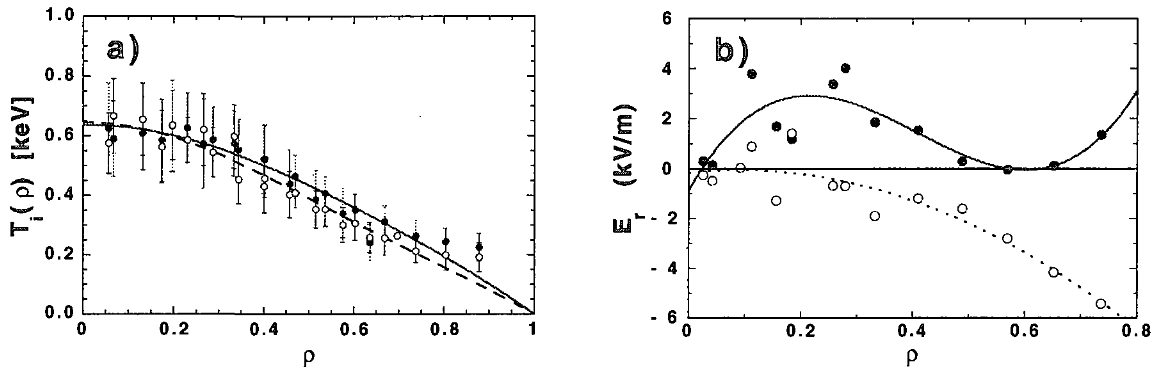

Fig. 4 (a) Ion Temperature and (b)Radial electric field obtained by CXRS measurement between t= 60 and 80 ms. The solid lines with closed circles show those for NBI+ECH-discharges, while the dashed lines with open circles do those for NBI-discharges.

During ECH-supeposed phase, the radial electric field turned to positive as shown in Fig.4(b). To see the effect of this E_r-change on the confinement of particles which are measured by NPA, orbit calculations are performed and the orbit following time are examined. The particles are launched from the sight line of NPA and the full-gyro motion is followed in the calculation. At each launching point, the particle is directed to the pivot point of NPA. The calculation is proceeded by reversing the time. Orbit following time are calculated for the particle having an energy of 1-, 2-, 5- and 8-keV. Electric Potentials: $\phi(\rho)$ are evaluated by integrating the measured E_r-profile along the radial direction with the boundary condition of $\phi(1)=0$. In the parallel sight line, almost all of the particles are confined and show closed drift surfaces. No electric field dependence of orbit following time are observed in this case. On the other hand, the orbit following time of perpendicular case is strongly depend on the choice of electric potential. The calculated

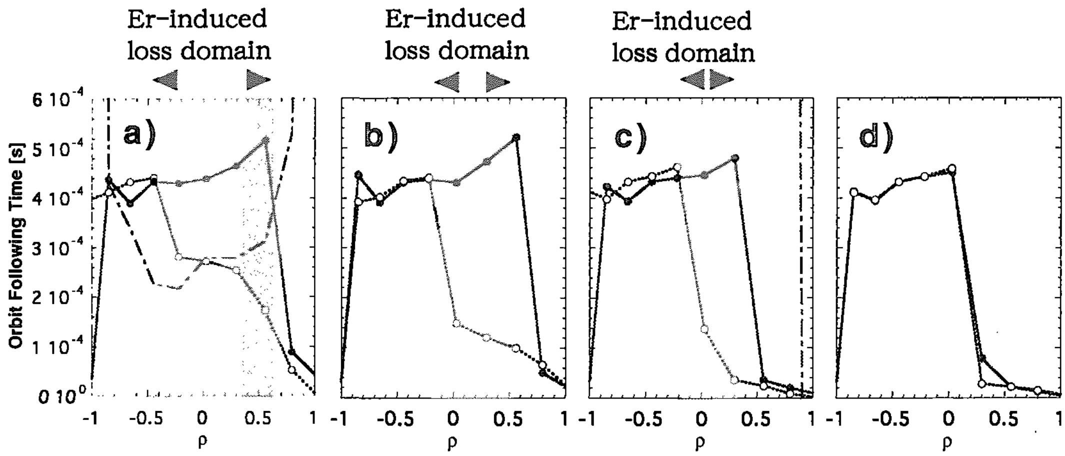

Fig. 5 Orbit following times of partices launched from the NPA perpendicular sight line. The energy of the Particles are (a)1keV, (b) 2keV, (c) 5keV, and (d) 8keV. Solid lines with closed cirdles represent the case where the electric potential profile of NBI+ECH-discharges are assumed, while dashed lines with open circles do the case where that of NBI-discharges are assumed. The center dashed lines show the path averaged collision time. The path averaged charge exchange loss time are also calculated, which are order of 1~10ms. The calculations are trancated at about 0.4ms.

orbit following time for perpendicular case are shown in Fig.5. A strong reduction of loss cone induced by the radial electric field are seen in the calculation with the particle energy of below 5-keV. When the particle energy is down below the 1-keV, the effect of E_r-field on the particle loss becomes weak. In this energy range, most of the particles which are on the prompt loss orbit are considered as confined particles, since the collision time becomes comparable to the orbit following time of the lost particles.

In summary, the effect of E_r-induced loss is significant between 1- and 5-keV with the E_r-field obtained at the experiments. This results is consistent with the result obtained by perpendicular NPA measurement.

Reference

[1] K. Uo, *et.al.*, Nucl. Fusion **22** (1982)1386

[2] H. Sanuki, *et.al.*, Journal of Phys. Soc. of Japan **62** (1993) 123

[3] K.Itoh, *et. al.*, Phys. Fluid B**3** (1991) 1295

[4] K.Hanatani, et. al., Nucl. Fusion **32** (1992) 1769

[5] S.Murakami, et. al., Nucl. Fusion **34** (1994) 913

[6] Kurimoto, *et.al.*, Fusion Engineering and Design **34,35** (1997) 539

[7] H. Zushi, *et.al.*, Fusion Engineering and Design **34,35** (1997) 527